



Ab initio and density functional theory studies on vibrational spectra of 3-[[[4-methoxyphenyl)methylene]amino]-2-phenylquinazolin-4(3H)-one

Chacko Yohannan Panicker^{a,b,*}, Hema Tresa Varghese^{b,c}, Kalappat Raman Ambujakshan^d, Samuel Mathew^e, Subarna Ganguli^f, Ashis Kumar Nanda^g, Christian Van Alsenoy^h and Sheena Mary Yohannanⁱ

^a Department of Physics, Thangal Kunju Musaliar College of Arts and Science, Kollam, Kerala, IN-691005, India

^b Department of Physics, Mar Ivanios College, Nalanchira, Trivandrum, Kerala, IN-695015, India

^c Department of Physics, Fatima Mata National College, Kollam, Kerala, IN-691001, India

^d Department of Physics, Muslim Educational Society Ponnani College, Ponnani South, Malappuram, Kerala, IN-679586, India

^e Department of Physics, Mar Thoma College, Thiruvalla, Kerala, IN-689103, India

^f Calcutta Institute of Pharmaceutical Technology and Allied Health Sciences, Banitabla, Uluberia, Howrah, IN-711316, India

^g Department of Chemistry, North Bengal University, Raja Rammohunpur, Siliguri, IN-734013, India

^h Chemistry Department, University of Antwerp, Universiteitsplein 1, Antwerp, B2610, Belgium

ⁱ Department of Physics, University College, Trivandrum, Kerala, IN-695034, India

*Corresponding author at: Department of Physics, Thangal Kunju Musaliar College of Arts and Science, Kollam, Kerala, IN-691005, India. Tel.: +91.989.5370968; fax: +91.474.2711817. E-mail address: cyphyp@rediffmail.com (C.Y. Panicker).

ARTICLE INFORMATION

Received: 27 February 2010

Received in revised form: 11 March 2010

Accepted: 15 March 2010

Online: 31 March 2010

KEYWORDS

Quinazoline

IR Spectra

Raman Spectra

DFT calculations

PED

ABSTRACT

The infrared and Raman spectra of 3-[[[4-methoxyphenyl)methylene]amino]-2-phenylquinazolin-4(3H)-one have been recorded and analysed. Geometry and harmonic vibrational wavenumbers were calculated theoretically using Gaussian 03 set of quantum chemistry codes. Calculations were performed at the Hartree-Fock and DFT (B3LYP) levels of theory using the standard 6-31G* basis. The calculated wavenumbers (B3LYP) agree well with the observed wavenumbers. The proposed assignments of normal modes are based on potential energy distribution (PED) analysis. Calculated infrared intensities and first hyperpolarizability are reported. The prepared compound was identified by NMR and mass spectra. The phenyl C-C stretching modes are equally active as strong bands in both IR and Raman spectra, which are responsible for hyperpolarizability enhancement leading to nonlinear optical activity. The calculated first hyperpolarizability is comparable with the reported values of similar structures and is an attractive object for further studies of nonlinear optics.

1. Introduction

Quinazolines and their derivatives play an important role in medicinal chemistry because of their wide range of biological activities [1,2]. Quinazoline derivatives exhibit antibacterial, antifungal, anti-HIV, anthelmintic, central nervous system depressant, antitubercular, hypotensive, anticonvulsant, anti-fibrillatory, diuretic, and antiviral activities [3-14]. Quinazolines are also used for the extraction and analytical determination of metal ions. The intramolecular imidate-amide rearrangement of 2-substituted 4-(chloroalkoxy)quinazoline derivatives have been reported by Chen *et al.* [15]. Sawunyama and Bailey [16] have reported the quantum mechanical study of the competitive hydration between protonated quinazoline and Li⁺, Na⁺ and Ca²⁺ ions. The authors have reported the vibrational spectroscopic and theoretical calculations of certain quinazoline derivatives [17,18]. Nonlinear optics deals with the interaction of applied electromagnetic fields in various materials to generate new electromagnetic fields, altered in wavenumber, phase, or other physical properties [19].

The present work deals with the study of FT-IR, FT-Raman, theoretical calculations of the wavenumbers and the hyperpolarizability of the title compound.

2. Experimental

The synthesis of the title compound was accomplished by condensation of 3-amino-2-phenylquinazolin-4-(3H)-one with *p*-methoxybenzaldehyde in methanol under thermal reflux for about 4 h [20]. Subsequently we found that the reaction took only about half an hour if the solvent methanol is not used. In this procedure equimolar amount of 3-amino-2-phenylquinazolin-4(3H)-one and *p*-methoxybenzaldehyde were titrated in a watch glass with a glass pestle and the mixture was transferred into a vial; the vial was heated in an oil bath for 30 min at about 80 °C. The product was found to be sufficiently pure for subsequent use. However, it was crystallized from ethanol for the present use. The TLC of the compound showed single spot in silica-gel plate at $R_f = 0.75$; eluent benzene:ethylacetate (7:3); iodine vapour was used as developer. The uncorrected melting point was found to be 140 °C. Mass spectra was recorded in an FAB, JEOL SX 102 mass spectrometer and NMR spectra were recorded on Bruker-Avance 300Mz FT-NMR spectrometer, CDCl₃ was used as solvent and TMS as internal standard; The peak assignments were done on the basis of correlation spectroscopy (COSY), total correlation spectroscopy (TOCSY) and HSQC spectra in addition to the normal ¹H and ¹³C spectra.

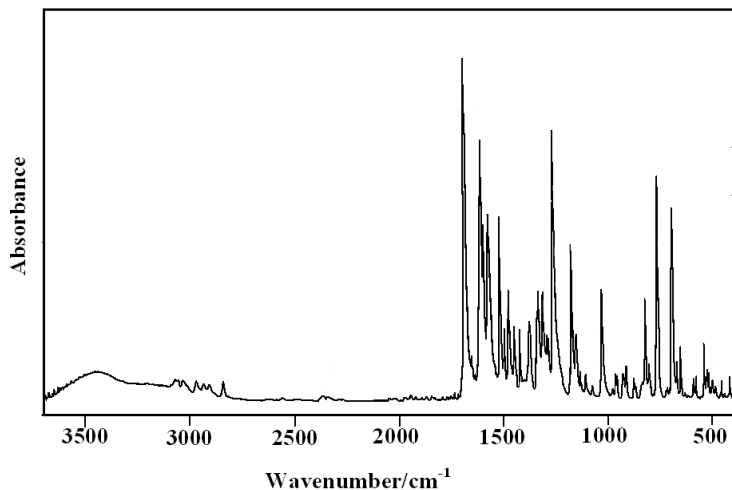


Figure 1. FT-IR spectrum.

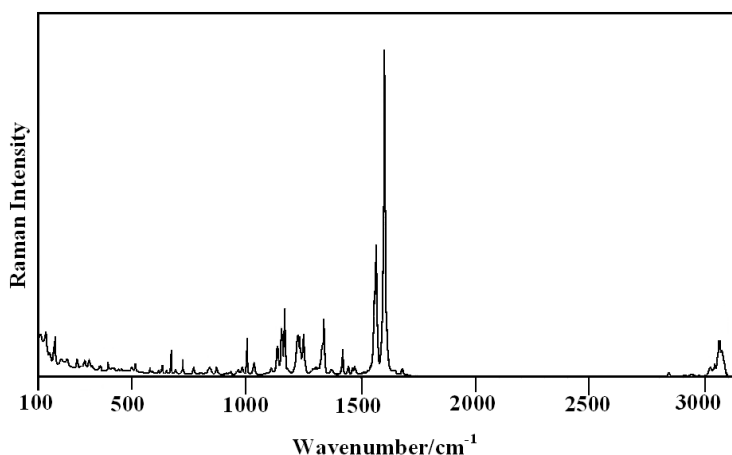


Figure 2. FT-Raman Spectrum.

The FT-IR spectrum (Figure 1) was recorded using a Bruker IFS 28 spectrometer with KBr pellets, number of scans 16, resolution 2 cm^{-1} . The FT-Raman spectrum (Figure 2) was obtained on a Bruker Equinox 55/s spectrometer with FRA Raman socket, 106/s. For excitation of the spectrum the emission of Nd:YAG laser was used, excitation wavelength 1064 nm, laser power 250 mW, resolution 2 cm^{-1} , number of scans 128, measurement on solid sample.

Yield 75 %. FAB MS (m/z): 356 ($M+1$). ^1H NMR: 3.84 (s, 3H, methoxy protons), 7.37 (H-36/H-38), 7.40 (H-27), 7.46 (H-9), 7.53 (H-7), 7.78 (H-26), 7.80 (H-10), 7.84 (H-32), 8.36 (H-8), 8.87 (1H, s, H-C=N-N). ^{13}C NMR: 55.40 (-O-CH₃), 114.34 (C-25), 121.48 (C-3), 125.89 (C-22), 126.90 (C-5), 127.26 (C-29), 127.70 (C-1), 127.88 (C-2), 129.89 (C-24), 129.90 (C-35), 130.75 (C-31), 134.79 (C-6), 134.67 (C-28), 146.50 (C-4), 159.40 (C-11), 163.08 (=C(OCH₃)-, C-23), 164.0 (C-14), 166.55 (H-C=N). Anal. Calcd.: for C₂₂H₁₇N₃O₂: C, 74.35, H, 4.82, N, 11.82; Found: C, 74.4, H, 4.90, N, 11.78 %.

3. Computational details

Calculations of the title compound were carried out with Gaussian03 software program [21] using the HF/6-31G* and B3LYP/6-31G* basis sets to predict the molecular structure and vibrational wavenumbers. At the optimized structure (Figure 3) of the examined species, no imaginary wavenumber modes were obtained, proving that a true minimum on the potential

surface was found. The DFT hybrid B3LYP functional tends also to overestimate the fundamental modes; therefore scaling factors have to be used for obtaining a considerably better agreement with experimental data. Therefore, a scaling factor of 0.9613 and 0.8929 were uniformly applied to the DFT and HF calculated wavenumbers [22]. The potential energy distribution (PED) is calculated with the help of GAR2PED software package [23].

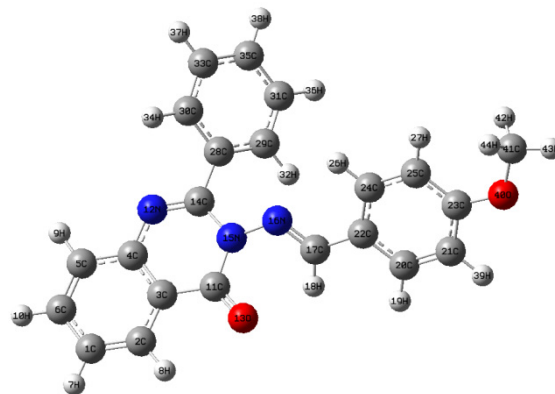


Figure 3. Optimized geometry of the molecule.

4. Results and Discussion

4.1. IR and Raman Spectra

The calculated (scaled) wavenumbers, observed IR and Raman bands with relative intensities and the assignments are shown in Table 1. In aromatic methoxy compounds, $\nu_{\text{as}}\text{CH}_3$ are expected in the region [24] of 2985 ± 20 and 2955 ± 20 cm^{-1} . The computed wavenumbers of modes corresponding to the $\nu_{\text{as}}\text{CH}_3$ group are 3032 and 2967 cm^{-1} . The bands observed at 3036, 2971 cm^{-1} in the IR spectrum and at 3018 cm^{-1} in the Raman spectrum was assigned as these modes. The symmetrical stretching mode $\nu_{\text{s}}\text{CH}_3$ is expected in the range of 2845 ± 45 cm^{-1} in which all the three CH bonds extend and contract in phase [24]. Theoretical calculations give a value of 2905 cm^{-1} for symmetrical methyl group stretching mode and the bands at 2909 cm^{-1} in IR are assigned as these modes. With methyl esters the overlap of the regions in methyl asymmetrical deformations are active (1465 ± 10 and 1460 ± 15 cm^{-1}) and quite strong, which leads to many coinciding wavenumbers [24]. This is obvious, not only for the asymmetric deformation, but also for the symmetric deformation [24] that is mostly displayed in the range of 1450 ± 20 cm^{-1} . The intensity of these adsorptions is only weak to moderate. The DFT calculations give 1459, 1447 and 1432 cm^{-1} as $\delta_{\text{as}}\text{CH}_3$ and $\delta_{\text{s}}\text{CH}_3$, respectively, for the title compound. The bands observed at 1474, 1447 cm^{-1} (IR) and 1473, 1446 cm^{-1} (Raman) are assigned as the deformation bands of the methyl group. The methyl rocking vibration [24] has been observed at 1190 ± 45 cm^{-1} . The second methyl rock [24] absorbs at 1150 ± 30 cm^{-1} . The bands calculated at 1164 and 1131 cm^{-1} were assigned as rocking modes of the methyl group. These modes are observed at 1173, 1134 in IR and at 1167, 1134 cm^{-1} in Raman spectra.

A methoxy group attached to an aromatic ring give $\nu_{\text{as}}\text{C-O-C}$ in the range of 1310-1210 cm^{-1} and $\nu_{\text{s}}\text{C-O-C}$ in the range [25] of 1050-1010 cm^{-1} . The DFT calculations give 1255 cm^{-1} and 1030 cm^{-1} as asymmetric and symmetric C-O-C stretching vibrations, respectively. The bands observed at 1259, 1030 cm^{-1} in IR and 1250, 1033 cm^{-1} in Raman spectrum, are assigned as C-O-C stretching vibrations. The skeletal C-O deformation can be found in the region [24] of 320 ± 50 cm^{-1} . Klimentova *et al.* [26] reported the asymmetric and symmetric C-O-C stretching vibrations in the range of 1214-1196 cm^{-1} and 1093-1097 cm^{-1} . Castaneda *et al.* [27] reported the methoxy vibrations at 1252, 1190, 1172, 1028 and 1011 cm^{-1} .

The carbonyl group is contained in a large number of different classes of compounds, for which a strong absorption band due to the C=O stretching vibration is observed in the region [28] of 1850-1550 cm^{-1} . For the title compound, the $\nu_{\text{C=O}}$ mode is seen as a strong band at 1683 cm^{-1} in the IR and at 1682 cm^{-1} in the Raman spectrum. The calculated value is 1690 cm^{-1} . For similar quinazoline derivatives [17,18] the $\nu_{\text{C=O}}$ mode is reported at 1652, 1673 cm^{-1} in the IR spectrum and at 1656, 1661 cm^{-1} in the Raman spectrum. The deformation bands of the C=O group are also identified (Table 1).

The C=N stretching skeletal bands [29-31] are observed in the range of 1650-1550 cm^{-1} . For the title compound the bands observed at 1561, 1540 cm^{-1} in the IR spectrum and at 1568 cm^{-1} in the Raman spectrum are assigned as $\nu_{\text{C=N}}$ modes. The DFT calculations give these modes at 1614, 1589, 1543 cm^{-1} and these modes are not pure but contain significant contribution from other modes. For conjugated azines the $\nu_{\text{C=N}}$ mode is reported [32] at 1553 cm^{-1} . We have reported the $\nu_{\text{C=N}}$ mode at 1662, 1652, 1588, 1546 cm^{-1} in the IR spectrum, 1656 cm^{-1} in Raman spectrum and at 1669, 1646, 1584, 1561, 1535 cm^{-1} theoretically [17,18].

Two bands are observed at 1360-1250 cm^{-1} and at 1280-1180 cm^{-1} for aromatic and unsaturated amines corresponding to $\nu_{\text{C-N}}$ [28]. Primary and secondary aromatic amines absorb

strongly in the first region. Primary aromatic amines with nitrogen directly on the ring absorb at 1330-1260 cm^{-1} because of the stretching of the phenyl C-N bond [25]. For the title compound, the $\nu_{\text{C}_4\text{-N}_{12}}$ stretching mode is observed at 1233 cm^{-1} in Raman and at 1266, 1229 cm^{-1} theoretically, as expected. From the PED calculations, it is seen that, these modes are not pure but contain significant contributions from other modes. The C-N stretching bands are reported in the range [33] of 1100-1300 cm^{-1} . In the present case, the $\nu_{\text{C}_{14}\text{-N}_{15}}$ and $\nu_{\text{C}_{11}\text{-N}_{15}}$ stretching bands are observed at 1308, 1110 cm^{-1} in the IR spectrum and at 1108 cm^{-1} in the Raman spectrum, and at 1297, 1104 cm^{-1} theoretically. For similar quinazoline derivatives, the C-N stretching modes are reported at 1109, 1232, 1246, 1273, 1283 cm^{-1} in the IR spectrum, 1243, 1250, 1286, 1295 cm^{-1} in the Raman spectrum and at 1110, 1119, 1235, 1240, 1248, 1257, 1283, 1288 cm^{-1} theoretically [17,18]. $\nu_{\text{N-N}}$ has been reported at 1115 cm^{-1} by Crane *et al.* [34] at 1121 cm^{-1} by Bezerra *et al.* [35] and at 1130 cm^{-1} by El-Behery and El-Twigry [36]. The band observed at 1119 (DFT) cm^{-1} is assigned to the $\nu_{\text{N}_{15}\text{-N}_{16}}$ mode. The N-N stretching mode is reported at 1093 cm^{-1} experimentally for quinazoline derivatives [18].

In the following discussion, the mono, ortho and para substituted phenyl rings and the quinazoline moiety are designated as PhI, PhII, PhIII and Ring, respectively. The C-H stretching occurs above 3000 cm^{-1} and is typically exhibited as a multiplicity of weak to moderate bands, compared to the aliphatic C-H stretching [37]. In the present case, the DFT calculations give $\nu_{\text{C-H}}$ modes of the phenyl rings in the range of 3057-3105 cm^{-1} . Corresponding to the $\nu_{\text{C}_{17}\text{-H}_{18}}$ mode, the DFT calculations give this mode at 3065 cm^{-1} with a PED contribution of 83%. The deformations bands of $\text{C}_{17}\text{-H}_{18}$ are also identified.

The benzene ring possesses six ring-stretching vibrations, of which the four with the highest wavenumbers (occurring near 1600, 1580, 1490 and 1440 cm^{-1}) are good group vibrations [24]. With heavy substituents, the bands tend to shift to somewhat lower wavenumbers. In the absence of ring conjugation [24], the band at 1580 cm^{-1} is usually weaker than that at 1600 cm^{-1} . In the case of C=O substitution, the band near 1490 cm^{-1} can be very weak [24]. The fifth ring stretching vibration is active near 1315 ± 65 cm^{-1} , a region that overlaps strongly with that of the CH in-plane deformation [24]. The sixth ring stretching vibration, or the ring breathing mode appears as a weak band near 1000 cm^{-1} in mono, 1,3-di- and 1,3,5-trisubstituted benzenes. In the otherwise substituted benzenes, however, this vibration is substituent sensitive and difficult to distinguish from the ring in-plane deformation [24]. The ν_{Ph} modes are expected in the region of 1615-1270, 1620-1285 and 1620-1260 cm^{-1} for PhI, PhII and PhIII rings, respectively [24]. The ν_{Ph} modes are observed at 1569, 1421 cm^{-1} in the IR spectrum, 1422, 1002 cm^{-1} in the Raman spectrum, in the range of 1593-1011 cm^{-1} theoretically for ring PhI; at 1604, 1561, 1540, 1454, 1340, 1183, 1079 cm^{-1} in the IR spectrum, 1602, 1568, 1339 cm^{-1} in the Raman spectrum and in the range of 1599-1086 cm^{-1} theoretically for ring Ph II and at 1591, 1550, 1515, 1495, 1330, 1259 cm^{-1} in the IR spectrum, 1250 cm^{-1} in the Raman spectrum and in the range of 1614-1255 cm^{-1} theoretically for ring PhIII. Due to aromatic ring vibrations quinazolines [30] absorb strongly at 1635-1610, 1580-1565 and 1520-1475 cm^{-1} .

In ortho di-substitution the ring breathing mode has three wavenumber intervals depending on whether both substituents are heavy, or one of them is heavy, while the other is light, or both of them are light. In the first case, the interval is 1100-1130 cm^{-1} , in the second case 1020-1070 cm^{-1} , while in the third case it is between [38] 630-780 cm^{-1} . The ring breathing modes of the phenyl rings are assigned at 1086, 1011, 854 cm^{-1} (DFT) by PED calculations. The ring breathing

Table 1. Calculated vibrational wavenumbers, measured infrared and Raman band positions and assignments for 3-[[[4-methoxyphenyl)methylene]amino]-2-phenylquinazolin-4(3H)-one.

HF/631G*		B3LYP/6-31G*		$\nu_{(IR)}$ (cm ⁻¹)	$\nu_{(Raman)}$ (cm ⁻¹)	Assignments, PED (%) ^a
ν (cm ⁻¹)	IR Intensity	ν (cm ⁻¹)	IR Intensity			
3059	0.90	3105	7.44			ν CH I (98)
3047	12.85	3102	9.73			ν CH III (99)
3046	10.41	3098	6.49			ν CH I (98)
3045	2.56	3097	13.12			ν CH II (93)
3043	6.74	3092	6.73			ν CH III (96)
3043	4.67	3091	10.34			ν CH II (100)
3042	16.83	3088	4.38			ν CH III (96)
3029	7.41	3079	31.04			ν CH I (92)
3023	17.21	3077	18.22	3071 w	3072 sh	ν CH II (100)
3022	44.90	3068	13.44			ν CH I (94)
3010	15.01	3065	7.43			ν CH III (15), ν C ₁₇ H ₁₈ (83)
3006	7.79	3062	5.93			ν CH II (98)
3001	10.38	3060	3.30		3061 m	ν CH III (78), ν C ₁₇ H ₁₈ (16)
2997	0.09	3057	0.03	3057 w	3038 w	ν CH I (97)
2986	31.75	3032	26.94	3036 w	3018 w	ν_{as} CH ₃ (90)
2928	45.33	2967	36.12	2971 w		ν_{as} CH ₃ (99)
2863	41.91	2905	63.24	2909 w		ν_s CH ₃ (100)
1664	224.68	1690	249.98	1683 vs	1682 w	ν C ₁₁ O ₁₃ (73)
1643	266.68	1614	11.02			ν C ₁₇ N ₁₆ (34), ν Ph III (34)
1623	188.48	1599	28.45	1604 s	1602 vs	ν Ph II (61)
1620	189.16	1593	3.15			ν Ph I (62)
1616	60.66	1589	402.85	1591 vs		ν Ph III (35), ν C ₁₇ N ₁₆ (24)
1598	297.05	1577	89.71	1569 s		ν Ph I (46), ν C ₁₄ N ₁₂ (13)
1584	208.68	1561	89.65	1561 w	1568 vs	ν Ph II (33), ν C ₁₄ N ₁₂ (34)
1579	62.70	1553	21.95	1550 w		ν Ph III (61)
1576	29.80	1543	261.58	1540 w		ν Ph II (18), ν C ₁₄ N ₁₂ (52)
1521	106.24	1501	83.31	1515 s		ν Ph III (24), ν C ₂₃ O ₄₀ (10), δ CH III (44)
1501	42.46	1479	15.10	1495 m		δ CH I (57), ν Ph III (32)
1483	9.03	1459	56.08	1474 s	1473 w	δ_{as} CH ₃ (86)
1478	65.45	1456	87.46	1454 w		δ CH II (42), ν Ph II (29), ν C ₄ N ₁₂ (13)
1467	6.43	1447	6.11	1447 m	1446 w	δ_{as} CH ₃ (93)
1483	9.03	1444	1.79			δ CH II (36), ν Ph II (27)
1454	10.44	1432	11.85			δ_s CH ₃ (84)
1449	13.58	1429	8.19	1421 m	1422 m	δ CH I (49), Ph I (27)
1420	1.33	1408	2.85			δ CH III (28), ν Ph III (49)
1390	18.10	1363	43.71	1373 m		δ N ₁₆ CC (45)
1343	9.59	1329	48.77	1340 w	1339 m	ν Ph II (85)
1328	75.63	1313	189.29	1330 s		ν Ph III (55)
1317	93.59	1310	23.09			δ CH I (32), ν Ph I (54)
1289	83.26	1297	70.42	1308 s		ν C ₁₄ N ₁₅ (43), ν C ₁₄ C ₂₈ (12)
1285	165.06	1295	11.35	1290 w		δ CH I (46), ν Ph I (29)
1262	398.82	1286	12.71	1283 w		δ CH III (66)
1245	22.97	1266	51.64			δ CH II (16), ν Ph I (12), ν C ₄ N ₁₂ (52), ν C ₁₄ N ₁₅ (12)
1237	11.49	1255	425.84	1259 vs	1250 m	ν Ph III (44), ν C ₂₃ O ₄₀ (41)
1234	21.97	1229	12.60		1233 sh	ν Ph II (15), δ CH II (27), ν C ₄ N ₁₂ (10), ν C ₃ C ₁₁ (11)
1224	5.11	1217	45.83		1224 m	ν C ₁₇ C ₂₂ (31), δ N ₁₆ CC (23)
1202	93.07	1201	11.65	1183 w		δ CH II (27), ν Ph II (20), ν C ₃ C ₁₁ (17)
1189	6.01	1164	9.36	1173 s	1167 s	δ CH I (77), ν Ph I (13)
1175	167.54	1164	8.19	1173 s	1167 s	δ HCO (57), δ CH ₃ (18)
1164	3.49	1149	157.12	1153 m	1154 m	δ CH III (67)
1159	3.20	1142	0.11			δ CH I (76), ν Ph I (13)
1150	26.09	1141	0.90			δ CH II (60)
1147	15.00	1131	0.67	1134 w	1134 w	δ HCO (24), δ CH ₃ (70)
1139	2.10	1119	27.69			δ CH II (35), ν N ₁₅ N ₁₆ (34)
1121	20.82	1104	7.41	1110 w	1108 w	ν C ₁₁ N ₁₅ (42), ν C ₁₄ N ₁₅ (13)
1109	2.41	1096	3.27			δ CH III (55), ν Ph III (20)
1100	22.97	1086	6.81	1079 w		δ CH II (25), ν Ph II (23), δ CCC III (18)
1078	4.88	1070	6.14			δ CH I (34), ν Ph I (48)
1063	0.32	1030	65.12	1030 s	1030 s	ν O ₄₀ C ₄₁ (76)
1056	0.19	1017	4.29			δ CH I (22), ν Ph I (65)
1048	11.65	1011	5.88		1002 m	δ CH II (25), ν Ph I (63)
1033	1.85	986	0.23	983 w		δ CCC III (47), ν Ph III (37)
1032	1032	978	1.90		981 w	δ CCC I (64), ν Ph I (22)
1029	0.96	963	0.01	967 w		γ CH II(88), τ CCCC II (11)
1024	6.89	961	0.28	958 w		γ CH I(73), τ CCCC I (14)
1016	47.51	955	16.58			γ CH ₁₈ (36), ν C ₁₁ N ₁₅ (21)
1012	20.32	947	3.62			γ CH ₁₈ (36), γ CH III (33)
1008	20.31	942	1.34			γ CH II (92)
1008	11.83	938	2.56	934 w		γ CH I (90)
998	1.20	936	0.61	927 w		γ CH III (85)
982	4.42	919	3.91	916 w		γ CH III (55), γ CH ₁₈ (14)
965	9.51	909	19.61			γ CH I (51), δ CCC II (20)
930	5.77	898	19.54	879 w		γ CH I (56), δ CCC II (22)
915	53.44	862	1.12		870 w	γ CH II (82)
882	1.32	854	7.29	840 w	841 w	δ CCC II (42), ν Ph III (31)
875	83.54	830	15.87			δ CCC II (28), ν Ph II (40)
863	0.38	824	3.73			γ CH I (96)
860	2.58	814	38.24	822 s		γ CH III (68), γ CO (13), τ CCCC III (10)
834	30.61	799	0.49	807 w		γ CH III (99)

Table 1 (Continued).

HF/631G*		B3LYP/6-31G*		$\nu_{(IR)}$ (cm ⁻¹)	$\nu_{(Raman)}$ (cm ⁻¹)	Assignments, PED (%) ^a
ν (cm ⁻¹)	IR Intensity	ν (cm ⁻¹)	IR Intensity			
829	20.77	765	6.82	772 s	771 w	γ CO (26), τ CCCC II (24), τ Ring (42)
807	39.33	764	2.48			δ CCC III (43), ν O ₄₀ C ₂₃ (25)
802	88.54	762	18.81	762 s		γ CH II (69)
761	4.92	755	45.63			τ CCCC II (21), δ CCC I (14), γ CH II (11), τ Ring (10)
746	20.26	708	2.72	718 w	722 w	τ CCCC III (57)
731	41.83	699	1.74		695 w	τ CCCC III(54), γ CO (13)
711	40.67	684	34.71	690 s		γ CH I (34), τ CCCC I (12), γ Ring (18)
707	5.93	677	6.52			τ CCCC I (59), γ CH I (20)
699	11.19	672	11.39	673 w	673 w	γ CH II (14), γ CO (34), τ CCCC II (25)
675	10.77	660	8.52	654 w	654 w	δ CCC I (34), δ CCC II (23), δ Ring (18)
659	19.92	645	16.55	640 w	634 w	δ CCC II (18), τ CCCC I (16), δ CO (12), δ Ring (16)
641	1.16	623	1.21	625 w	620 w	δ CCC III (71)
626	0.10	608	0.19	593 w		δ CCC I (81)
584	0.49	571	5.71	580 w		δ CCC II (44), δ CCC III (32)
570	21.64	567	11.08		567 w	δ Ring (37), δ CCC II (35)
557	14.82	534	6.97	540 m		τ CCCC II (47), γ CH II (14), τ Ring (13)
545	7.19	523	5.32	527 w		γ CO (28), τ CCCC III (27), γ C ₁₇ (21)
520	7.97	509	7.48	517 w	517 w	δ Ring (44), δ CH ₃ (38)
508	3.17	502	3.77	502 w	500 w	δ Ring (26), δ CCC II (10), δ CO (24)
486	5.23	473	3.54	488 w	478 w	τ CCCC I (48), γ Ring (42)
461	1.49	447	9.02	457 w	446 w	τ CCCC I (24), τ CCCC II (30), δ Ring (22)
437	49.18	432	16.53			τ CCCC II (37), δ CNN (26)
432	1.38	416	0.88	417 w		τ CCCC III (45), τ CCCC II (18)
420	1.02	414	2.45			τ CCCC III (36), δ CCC III (22), δ Ring (21)
416	1.06	403	0.73			τ CCCC III (47), τ CCCC II (18), τ CCCC I (12)
409	0.75	400	0.01		398 w	τ CCCC I (74)
363	4.83	4.83	3.07		362 w	τ CCCC II (24), δ CO (21), δ Ring (30)
330	0.66	318	0.92		315 w	τ CCCC II (25), δ Ring (18), τ Ring (14)
312	19.49	304	11.66		294 w	γ Ring (40), γ C ₁₇ (20), CNNC (26)
281	5.02	277	5.36			δ Ring (26), τ CCCC I (24), τ CCCC II (22)
268	0.52	271	0.04			τ CCCC I (20), γ Ring (12), δ CH ₃ (13), δ CO (11)
247	2.39	257	1.87		263 w	τ CNNC (23), δ CO (26), δ Ring (20)
221	0.52	238	1.25			τ OCH ₃ (56), γ Ring (10), τ CNNC (12)
208	0.76	214	0.66		219 w	δ CO (13), γ Ring (18), τ Ring (16), τ CCCC I (18)
203	0.20	203	0.29		203 w	δ CCC ₁₄ (23), τ Ring (29), τ CCCC III (24)
183	1.47	200	2.89			τ CNNC (40), τ CCCC III (24), τ Ring (20)
158	7.34	160	2.68		170 m	τ CNNC (38), τ Ring (28), δ CNN (22)
137	1.44	134	2.19			τ Ring (20), τ CCCO (14), τ CCCC II (14), τ CCCC III (12)
127	2.14	122	2.32		129 m	τ Ring (28), τ CCCO (19), τ CNNC (18)
88	18.44	95	5.30			τ CCCO (38), τ OCH ₃ (20), τ Ring (25)
81	3.20	81	1.54			τ CNNC (17), δ NCC (19), γ C ₁₄ (10), τ Ring (10)
67	1.38	73	0.22			τ CCCO (30), τ OCH ₃ (14), τ CCCC III (14), τ Ring (15)
52	0.61	51	0.34			τ Ring (25), γ Ring (19), γ C ₁₄ (14)
45	0.50	48	0.31			τ Ring (66), δ NCC (12)
32	0.17	34	0.08			τ CNNC (58), δ C ₁₇ C (12)
23	1.73	23	1.19			τ Ring (57), δ CNN (29)
14	0.44	17	0.32			τ Ring (44), δ CNN (39)

^a ν -Stretching, δ -in-plane bending, γ -out-of-plane bending, τ -torsion, s-strong, m-medium, w-weak, v-very, br-broad; mono, ortho and para substituted phenyl rings are designated as PhI, PhII and PhIII; Ring, quinazoline ring; PED, potential energy distribution, only contribution larger than 10% were given

modes [38] for the para substituted benzenes with entirely different substituents have been reported in the interval of 780 - 840 cm⁻¹ in the IR spectrum. For the title compound, this is confirmed by the band in the infrared spectrum at 840 cm⁻¹, which finds support from the computational results. Ambujakshan *et al.* [39] reported a value of 792 (IR) and 782 cm⁻¹ (theoretical) as the ring breathing mode of para substituted benzenes. The in-plane and out-of-plane CH deformations of the phenyl ring are expected above and below 1000 cm⁻¹, respectively [24]. Generally, the CH out-of-plane deformations with the highest wavenumbers have a weaker intensity than those absorbing at lower wavenumbers. According to Roeges [24] in the case of 1,2-disubstitution only one strong absorption in the region of 755 \pm 35 cm⁻¹ is observed, and is due to γ CH mode. This is confirmed by the presence of a strong γ CH at 762 cm⁻¹ in the IR spectrum and is supported by the computation result at 762 cm⁻¹. The γ CH mode at 690 cm⁻¹ and ring deformation at 654 cm⁻¹ in the IR spectrum form a pair of characteristic bands of mono substituted benzene derivatives [24]. The strong γ CH deformation occurring at 840 \pm 50 cm⁻¹ is typical for para substituted benzene derivatives [24], and this band is observed

at 822 cm⁻¹ in the IR spectrum and at 814 cm⁻¹ theoretically. Most of the deformation bands of the CH vibrations of the phenyl rings are not pure but contain significant contributions from other modes (Table 1). The IR bands in the region of 2840-2361 cm⁻¹ and their large broadening support the intramolecular hydrogen bonding [40].

4.2 Geometrical parameters and first hyperpolarizability

The theoretical results obtained are almost comparable with the reported structural parameters of the parent quinazoline molecules. For the title compound, the bond lengths of the methoxy group C₂₃-O₄₀=1.3865 Å and O₄₀-C₄₁=1.4532 Å, whereas the reported values of similar derivatives are 1.350 Å (DFT), 1.3245 Å (XRD) and 1.442 Å (DFT), 1.4376 Å (XRD) [41]. Filarowski *et al.* [42] reported the corresponding values as 1.3422 Å (XRD), 1.3391 Å (DFT) and 1.4473 Å (XRD), 1.4306 Å (DFT) and Castneda *et al.* [27] reported these values in the range 1.3553-1.3574 Å and 1.4154-1.4404 Å. The reported values of the bond angles C₂₃-O₄₀-C₄₁=115.8° (DFT), 116.0° (XRD) [41], 118.4° (XRD), 119.5° (DFT) [42], 117.5-118.0° (XRD), 118.9-119.0° [27], O₄₀-C₂₃-C₂₅ =

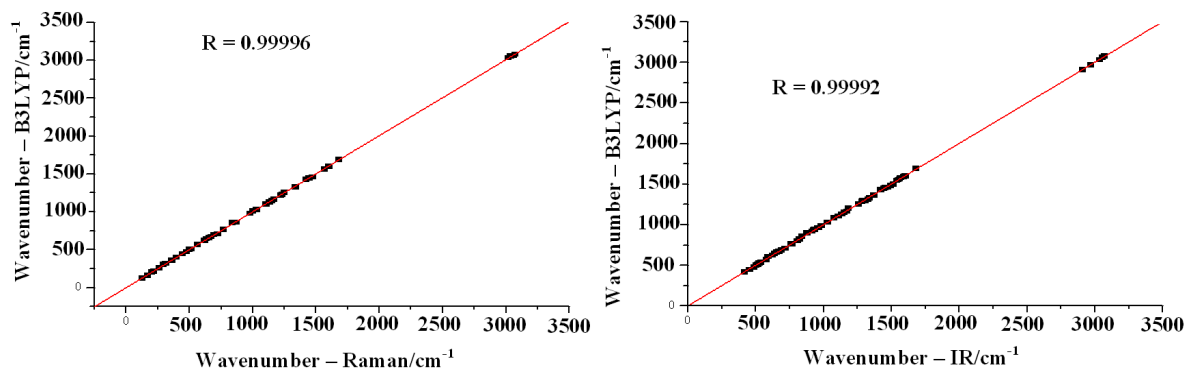


Figure 4. Correlation graph between experimental and computed wavenumbers.

124.2° (XRD), 123.3° (DFT) [42], 124.0° (DFT) [27] and O₄₀-C₂₃-C₂₁=118.1° (XRD), 118.3° (DFT) [42], 116.0° [27] whereas for the title compound the corresponding values are 119.1, 124.3 and 115.5°, respectively. For the title compound the dihedral angles of the methoxy group are, C₂₁-C₂₃-O₄₀-C₄₁= -179.5°, C₂₀-C₂₁-C₂₃-O₄₀= 179.9°, C₂₄-C₂₅-C₂₃-O₄₀= -179.8°, C₂₅-C₂₃-O₄₀-C₄₁=0.4° where as the reported values are C₂₁-C₂₃-O₄₀-C₄₁= -180.0° [41], -177.9° [41], -176.9° [27], C₂₀-C₂₁-C₂₃-O₄₀= -179.6° [42], C₂₄-C₂₅-C₂₃-O₄₀= -176.8° [42], C₂₅-C₂₃-O₄₀-C₄₁= -0° [42], 3.28° [27].

The asymmetry of the exocyclic angles O₄₀-C₂₃-C₂₁=115.5° and O₄₀-C₂₃-C₂₅=124.3° is more at C₂₃ position which gives highest repulsion of methyl group with the phenyl ring III. The computed values of above mentioned angles correlate well with reported results [43].

The experimental bond length of hydrazine [44] is reported at 1.449 Å and the electron diffraction N-N bond length of tetramethylhydrazine [45] is reported at 1.401 Å. Kostava *et al.* [46] calculated N₁₅-N₁₆ bond length in the range of 1.318-1.357 Å for different molecules. In the present case, the N₁₅-N₁₆ bond length is 1.4077 Å, which is somewhere between the length of an N-N single bond (1.45 Å) and an N=N double bond (1.25 Å). For similar derivatives, we have reported N-N bond lengths as 1.3892 [17] and 1.4033 Å [18] theoretically.

For quinazoline derivatives, the reported values of the bond lengths are C₁₄=N₁₂=1.2805 Å [17], 1.3078 Å [18], C₁₁=O₁₃= 1.2302 Å [17], 1.2535 Å [18], C₄-N₁₂= 1.3871 Å [17], 1.3902 Å [18], C₁₁-N₁₅= 1.3939 Å [17], 1.4268 Å [18] and C₁₄-N₁₅= 1.4037 Å [17], 1.4204 Å [18]. For the title compound, C₁₇=N₁₆=1.3014 Å, C₁₄=N₁₂=1.3090 Å and C₁₁=O₁₃= 1.2538 Å show typical double bond characteristics. However, the C₄-N₁₂=1.3896 Å, C₁₁-N₁₅=1.4263 Å and C₁₄-N₁₅=1.4178 Å bond lengths are shorter than the normal C-N single bond length of about 1.48 Å. The shortening of the C-N bonds reveal the effects of resonance in this part of the molecule [47]. The differences between the lengths of CN bonds are similar to the values of reported quinazoline derivatives [48] and this situation can be attributed to the difference in hybridization of the different carbon atoms.

For a quinazoline derivative, Costa *et al.* [49] reported C₄-N₁₂=1.3954 Å, C₁₄-N₁₅=1.3904 Å and C₁₁-N₁₅=1.4174 Å. Gai *et al.* [50] reported C₁₁-N₁₅, C₁₄-N₁₅, C₄-N₁₂, C₃-C₁₁ and C₄-C₃ as 1.3703, 1.4623 Å, 1.4043 Å, 1.4823 Å and 1.3903 Å, respectively, for a quinazoline derivative. In the present case, the corresponding values are 1.4261 Å, 1.4178 Å, 1.3896 Å, 1.4593 Å and 1.4124 Å, respectively. For the title compound, the B3LYP calculations give the bond angles, C₁₁-N₁₅-N₁₆=123.9°, C₁₁-N₁₅-C₁₄=121.2°, N₁₆-N₁₅-C₁₄= 114.3°, O₁₃-C₁₁-N₁₅=121.4°, O₁₃-C₁₁-C₃=123.4°, N₁₅-C₁₁-C₃=115.2°, C₄-C₃-C₂= 120.2°, C₄-C₃-C₁₁=119.6°, C₂-C₃-C₁₁= 120.2°, C₃-C₄-C₅= 119.5°, C₃-C₄-N₁₂= 121.2°, C₅-C₄-N₁₂= 119.2°, whereas the reported values [50] are 120.3, 121.0, 118.0, 121.8, 122.7, 115.5, 119.7, 120.6, 119.6, 120.0, 118.6 and 121.2° and the calculated values are in

agreement with the results reported previously by the authors [17,18].

The dihedral angles are C₂-C₃-C₁₁-N₁₅= -177.6° and C₁₁-N₁₅-C₁₄-C₂₈= -173.2°. This indicates that the phenyl ring II and the quinazoline moiety of the title compound are in tilted positions. Also the dihedral angles C₃₁-C₂₉-C₂₈-C₁₄, C₂₈-C₁₄-N₁₂-C₄ and C₂₈-C₁₄-N₁₅-C₁₁ are 175.2, 177.6 and -173.2°, respectively, which show the phenyl ring I and the quinazoline moiety are in different planes.

The N₁₆-C₁₇ moiety is essentially planar as seen from the torsion angles, N₁₆-C₁₇-C₂₂-C₂₀= -178.9° and N₁₆-C₁₇-C₂₂-C₂₄=1.0°. The N₁₂-C₁₄ ring moiety is slightly twisted from the phenyl ring II (C₃-C₄-N₁₂-C₁₄= -2.9° and C₅-C₄-N₁₂-C₁₄=178.4°) and more twisted from the phenyl ring I (N₁₂-C₁₄-C₂₈-C₂₉= -139.9° and N₁₂-C₁₄-C₂₈-C₃₀=39.7°) as is evident from the torsion angles. For a quinazoline derivative, Krishnakumar and Muthunatesan [51] reported the bond lengths N₁₂-C₁₄, N₁₅-C₁₄, C₁₁-C₃, C₃-C₂, C₂-C₁, C₁-C₆, C₆-C₅, C₅-C₄ as 1.311, 1.362, 1.427, 1.414, 1.380, 1.415, 1.380 and 1.416 Å. In the present case, the corresponding values are 1.309, 1.4178, 1.4593, 1.4082, 1.3895, 1.4118, 1.3891 and 1.4098 Å, respectively. The DFT calculations give the bonds angles of N₁₂-C₁₄-N₁₅, C₁₄-N₁₅-C₁₁, N₁₅-C₁₁-C₃, C₁₁-C₃-C₂, C₃-C₂-C₁, C₂-C₁-C₆, C₁-C₆-C₅, C₆-C₅-C₄ as 122.1, 121.2, 115.2, 120.2, 119.7, 120.1, 120.6, 119.8°, respectively, whereas the corresponding reported values are 127.7, 116.2, 123.4, 124.4, 119.5, 120.5, 120.9 and 126.1°, respectively [51].

The three bond angles around C₁₁ atom are not equal to 120° each. It is seen that the N₁₅-C₁₁-O₁₃ bond angle (121.4°) is considerably greater than N₁₅-C₁₁-C₃ angle (115.2°). This observation is similar to those in the structures of hydrazones reported earlier [52], which is explained as due to a decrease in the repulsion between the lone pairs present in N₁₅ and O₁₃ atoms.

The central part of the molecule adopts a completely extended double bonded conformation. It can be confirmed by the C₁₁-O₁₃ bond length (1.2538 Å) which is considerably larger than the standard C=O bond length of 1.21 Å and N₁₅-C₁₁ bond length of 1.4261 Å which is shorter than the standard N-C single bond length (1.47 Å) [52].

The calculated first hyperpolarizability of the title compound is 6 × 10⁻³⁰ esu, which is comparable with the reported values of similar derivatives [17,18] and experimental evaluation of this data is not readily available. We conclude that the title compound is an attractive object for future studies of non linear optical properties.

The correlation graph between the observed and calculated wavenumbers is given in Figure 4. RMS values of wavenumbers were evaluated using the following expression [53].

$$RMS = \sqrt{\frac{1}{n-1} \sum_i^n (v_i^{calc} - v_i^{exp})^2}$$

The RMS error of the observed Raman bands and IR bands are found to be 27.18, 33.55 for HF and 7.44, 8.19 for B3LYP methods, respectively. The small differences between experimental and calculated vibrational modes are observed. It must be due to the fact that hydrogen bond vibrations present in the crystal lead to strong perturbation of the infrared wavenumbers and intensities of many other modes. Also, we state that experimental results belong to solid phase and theoretical calculations belong to gaseous phase.

5. Conclusion

The HF and DFT calculations carried out using standard 6-31G* basis set give a reasonable fit for bands assigned experimentally. The calculated geometry of the title compound is in good agreement with that obtained from XRD and Computational data for similar compounds. Analyses of the phenyl ring modes show that C-C stretching mode is equally strong in both IR and Raman spectra, which can be interpreted as the evidence of intramolecular charge transfer via conjugated path, which is responsible for hyperpolarizability enhancement leading to nonlinear optical activity.

References

- [1]. Al-Omar, M. A.; Abdel-Hamide, S. G.; Alkhamees, H. A.; El-Subbagh, H. I. *Saudi Pharm. J.* **2004**, *12*, 63-71.
- [2]. Zia-Ur-Rehman, M.; Choudary, J. A.; Ahmad, S.; Siddiqui, H. L. *Chem. Pharm. Bull.* **2006**, *54*, 1175-1178.
- [3]. Alagarsamy, V.; Giridhar, R.; Yadav, H. R.; Revathi, R.; Rukmani, K.; De Clercq, E. *Indian J. Pharm. Sci.* **2006**, *68*, 532-535.
- [4]. Srivastava, V. K.; Singh, A.; Gucati, A.; Shankar, K. *Indian J. Chem.* **1987**, *26*, 652-656.
- [5]. Gupta, D. P.; Ahmed, S.; Kumar, A.; Shankar, K. *Indian J. Chem.* **1988**, *27*, 1060-1062.
- [6]. Jatav, V.; Mishra, P.; Kashaw, S.; Stables, J. P. *Eur. J. Med. Chem.* **2008**, *43*, 135-141.
- [7]. Joshi, V.; Chaurasia, R. P. *Indian J. Chem.* **1987**, *26*, 602-604.
- [8]. Prouse, I. R. (Ed.), *Drugs Future* **1993**, *18*, 475-485.
- [9]. Bhandari, S. V.; Deshmane, B. J.; Dangare, S. C.; Gore, S. T.; Raparti, V. T.; Khachane, C. V.; Sarkate, A. P. *Pharmacologyonline* **2008**, *2*, 604-613.
- [10]. Bekhit, A. A.; Habib, N. S.; Bekhit, A.; el-Din, A. *Bull. Chim. Farm.* **2001**, *140*, 297-301.
- [11]. Azza, M. R.; Eman, E. R.; Fatma, G. E. *Arch. Pharm.* **2004**, *337*, 527-532.
- [12]. Pandey, V. K.; Mishra, D.; Sukla, S. *Indian Drugs* **1994**, *31*, 532-536.
- [13]. Pandey, V. K. *Indian Drugs* **1988**, *25*, 168-172.
- [14]. Pandey, V. K.; Gupta, M.; Mishra, D. *Indian Drugs* **1996**, *33*, 409-411.
- [15]. Chen, G. S.; Kalchar, S.; Kuo, C. W.; Chang, C. S.; Usifoh, C. O.; Chern J. W. *J. Org. Chem.* **2003**, *68*, 2502-2505.
- [16]. Sawunyama, P.; Bailey, G. W. *J. Phys. Chem. A*, **2001**, *105*, 9717-9724.
- [17]. Panicker, C. Y.; Varghese, H. T.; Ambujakshan, K. R.; Mathew, S.; Ganguli, S.; Nanda, A.K.; Van Alsenoy, C. *J. Raman Spectrosc.* **2009**, *40*, 1262-1273.
- [18]. Panicker, C. Y.; Ambujakshan, K. R.; Varghese, H. T.; Mathew, S.; Ganguli, S.; Nanda, A. K.; Van Alsenoy, C. *J. Raman Spectrosc.* **2009**, *40*, 527-536.
- [19]. Shen, Y. R.; *The Principles of Nonlinear Optics*, Wiley, New York, 1984
- [20]. Nanda, A. K.; Ganguli, S.; Chakraborty, R. *Molecules* **2007**, *12*, 2413-2426.
- [21]. Frisch, M.; Trucks, G. W.; Schlegel, H. B.; Scuseria, G. E.; Robb, M. A.; Cheeseman, J. R.; Montgomery, Jr., J. A.; Vreven, T.; Kudin, K. N.; Burant, J. C.; Millam, J. M.; Iyengar, S. S.; Tomasi, J.; Barone, V.; Mennucci, B.; Cossi, M.; Scalmani, G.; Rega, N.; Petersson, G. A.; Nakatsuji, H.; Hada, M.; Ehara, M.; Toyota, K.; Fukuda, R.; Hasegawa, J.; Ishida, M.; Nakajima, T.; Honda, Y.; Kitao, O.; Nakai, H.; Klene, M.; Li, X.; Knox, J. E.; Hratchian, H. P.; Cross, J. B.; Adamo, C.; Jaramillo, J.; Gomperts, R.; Stratmann, R. E.; Yazyev, O.; Austin, A. J.; Cammi, R.; Pomelli, C.; Ochterski, J. W.; Ayala, P. Y.; Morokuma, K.; Voth, G. A.; Salvador, P.; Dannenberg, J. J.; Zakrzewski, V. G.; Dapprich, S.; Daniels, A. D.; Strain, M. C.; Farkas, O.; Malick, D. K.; Rabuck, A. D.; Raghavachari, K.; Foresman, J. B.; Ortiz, J. V.; Cui, Q.; Baboul, A. G.; Clifford, S.; Cioslowski, J.; Stefanov, B. B.; Liu, G.; Liashenko, A.; Piskorz, P.; Komaromi, I.; Martin, R. L.; Fox, D. J.; Keith, T.; Al-Laham, M. A.; Peng, C. Y.; Nanayakkara, A.; Challacombe, M.; Gill, P. M. W.; Johnson, B.; Chen, W.; Wong, M. W.; Gonzalez, C.; J. A. Pople, J. A. *Gaussian 03, Revision C.02 Gaussian*, Wallingford, 2004.
- [22]. Foresman, J. B.; *Exploring Chemistry with Electronic Structure Methods: A Guide to Using Gaussian*, Editor: E. Frisch, Gaussian, Pittsburg, PA, 1995.
- [23]. Martin, J. M. L.; Van Alsenoy, C. GAR2PED, A Program to obtain a Potential Energy Distribution from a Gaussian archive record, University of Antwerp, Belgium, 2007.
- [24]. Roeges, N. P. G.; *A Guide to the Complete Interpretation of Infrared Spectra of Organic Compounds*, Wiley, New York 1994.
- [25]. Colthup, N. B.; Daly, L. H.; Wiberly, S. E. *Introduction to Infrared and Raman Spectroscopy*, Academic Press, New York 1990.
- [26]. Klimentova, J.; Vojtisek, P.; Sklenarova, M. *J. Mol. Struct.* **2007**, *871*, 33-41.
- [27]. Castaneda, I. C. H.; Jios, J. L.; Piro, O. E.; Tobon, G. E.; Vedova, C. O. D. *J. Mol. Struct.* **2007**, *842*, 46-54.
- [28]. Socrates, G.; *Infrared Characteristic Group Frequencies*, John Wiley, New York, 1981.
- [29]. Silverstein, R. M.; Webster, F. X. *Spectrometric Identification of Organic Compounds*, ed.6, Wiley, Asia 2003.
- [30]. Yalcin, I.; Sener, E.; Ozden, O.; Akin, A. *Eur. J. Med. Chem.* **1990**, *25*, 705-708.
- [31]. Saxena, R.; Kandpaul, L. D.; Mathur, G. N. *J. Polym. Sci. Part A. Polym. Chem.* **2002**, *40*, 3959-3966.
- [32]. Engasser, J. M.; Horvath, C. *Biochem. J.* **1975**, *145*, 431-435.
- [33]. Kundoo, S.; Banerjee, A. N.; Saha, P.; Chattopadhyay, K. K. *Mater. Lett.* **2003**, *57*, 2193-2197.
- [34]. Crane, L. G.; Wang, D.; Sears, L. M.; Heyns, B.; Carron, K. *Anal. Chem.* **1995**, *67*, 360-364.
- [35]. Bezerra, A. C. S.; De Sa, E. L.; Nart, F. C. *J. Phys. Chem.* **1997**, *101B*, 6443-6449
- [36]. El-Beheri, M.; El-Twigry, H. *Spectrochim. Acta* **2007**, *66A*, 28-36.
- [37]. Coates, J.; in: *Encyclopedia of Analytical Chemistry; Interpretation of Infrared Spectra, A Practical Approach*, Editor: Meyers, R. A. John Wiley and Sons, Chichester, 2000.
- [38]. Varsanyi, G. *Assignments of Vibrational Spectra of Seven Hundred Benzene derivatives*, Wiley; New York, 1974.
- [39]. Ambujakshan, K. R.; Madhavan, V. S.; Varghese, H. T.; Panicker, C. Y.; Temiz-Arpaci, O.; Tekiner-Gulbaz, B.; Yildiz, I. *Spectrochim. Acta* **2008**, *69A*, 782-788.
- [40]. Philip, D.; John, A.; Panicker, C. Y.; Varghese, H. T. *Spectrochim. Acta* **2001**, *57A*, 1561-1566.
- [41]. Kanopacka, A.; Pawelka, Z. *J. Mol. Struct.* **2007**, *844-845*, 250-258.
- [42]. Filarowski, A.; Kochel, A.; Hancen, P. E.; Urbanowicz, A.; Szymorska, K. *J. Mol. Struct.* **2007**, *844-845*, 77-82.
- [43]. Bujak, M.; Zaleski, J.; Prezhdo, V.; Uspenskiy, B. *Acta Cryst.* **2002**, *C58*, o76-o77.
- [44]. Kohata, K.; Fukuyama, T.; Kuchitsu, K. *J. Phys. Chem.* **1982**, *86*, 602-606.
- [45]. Naumov, V. A.; Litvionov, O. A. *J. Mol. Struct.* **1983**, *99*, 303-307.
- [46]. Kostava, I.; Peica, N.; Kiefer, W. *J. Raman Spectrosc.* **2007**, *38*, 1-10.
- [47]. Arslan, H.; Florke, U.; Kulcu, N.; Binzet, G. *Spectrochim. Acta* **2007**, *68A*, 1347-1355.
- [48]. Candan, M. M.; Kendi, E.; Yarin, M.; Sarac, S.; Ertan, M. *Anal. Sci.* **2001**, *17*, 1023-1024.
- [49]. Costa, M.; Ca, N. D.; Gabriele, B.; Massera, C.; Salerno, G.; Soliani, M. *J. Org. Chem.* **2004**, *69*, 2469-2477.
- [50]. Gai, Z.; Qing, L. T.; Lan, S. H.; Hai, S. W.; She, Z. J.; Zhi-An, G. *Chin. Struct. Chem.* **2005**, *24*, 783-788.
- [51]. Krishnakumar, V.; Muthunatesan, S. *Spectrochim. Acta* **2007**, *66A*, 1082-1090.
- [52]. Raj, B. N. B.; Kurup, M. R. P.; Suresh, E. *Spectrochim. Acta* **2008**, *71A*, 1253-1260.
- [53]. Ushakumari, L.; Varghese, H. T.; Panicker, C. Y.; Ertan, T.; Yildiz, I. *J. Raman Spectrosc.* **2008**, *39*, 1832-1839.